



## Synthesis and evaluation of benzofuran-2-yl(phenyl)methanone derivatives as ligands for $\beta$ -amyloid plaques

Mengchao Cui<sup>a,b</sup>, Masahiro Ono<sup>a,\*</sup>, Hiroyuki Kimura<sup>a</sup>, Boli Liu<sup>b</sup>, Hideo Saji<sup>a,\*</sup>

<sup>a</sup> Graduate School of Pharmaceutical Sciences, Kyoto University, 46-29 Yoshida Shimoadachi-cho, Sakyo-ku, Kyoto 606-8501, Japan

<sup>b</sup> Key Laboratory of Radiopharmaceuticals, Ministry of Education, College of Chemistry, Beijing Normal University, Beijing 100875, PR China

### ARTICLE INFO

#### Article history:

Received 3 March 2011

Revised 26 April 2011

Accepted 26 April 2011

Available online 3 May 2011

#### Keywords:

Alzheimer's disease

$\beta$ -Amyloid

Imaging agent

Binding assay

Autoradiography

### ABSTRACT

A series of benzofuran-2-yl(phenyl)methanone derivatives were synthesized and evaluated as novel probes for  $\beta$ -amyloid plaques. These derivatives were produced by a Rap–Stoermer condensation reaction. Compounds with a *N,N*-dimethylamino group displayed high affinity for  $A\beta_{1-42}$  aggregates with  $K_d$  values in the nanomolar range. Autoradiography with brain sections of AD model mice (APP/PS1) revealed that a radioiodinated probe, [<sup>125</sup>I]**10**, labeled  $\beta$ -amyloid plaques selectively and displayed good brain uptake (3.53% ID/g) at 2 min. The results suggest that benzofuran-2-yl(phenyl)methanone derivatives should be investigated further as potential probes for detecting  $\beta$ -amyloid plaques in the AD brain.

© 2011 Elsevier Ltd. All rights reserved.

### 1. Introduction

Alzheimer's disease (AD) is a progressive brain disorder that causes problems with memory, thinking and behavior. Although the etiology of AD is not completely understood,  $\beta$ -amyloid ( $A\beta$ ) plaques and neurofibrillary tangles (NFTs) found in the brain are the best known histological hallmarks of the disease.<sup>1–3</sup> A clinical diagnosis based on neurological examinations and clinical history is often difficult and unreliable, and a definite diagnosis can only be made by post-mortem investigation to detect  $A\beta$  plaques in brain tissue. However, noninvasive functional imaging techniques such as positron emission tomography (PET) and single photon emission computed tomography (SPECT) together with specific

*in vivo* imaging agents targeting  $A\beta$  plaques would allow a more accurate diagnosis of AD.<sup>4,5</sup>

Over recent years, great efforts have been made to develop radiotracers that specifically bind to  $A\beta$  plaques *in vivo* (Fig. 1). [<sup>11</sup>C]PIB (2-(4'-[<sup>11</sup>C]methylaminophenyl)-6-hydroxybenzothiazole), a neutral Thioflavin T (ThT) derivative widely used as a PET radioligand for amyloid imaging, clearly distinguishes between AD and control cases.<sup>6,7</sup> Currently, a fluorine-18-labeled PIB analogue, [<sup>18</sup>F]GE-067 ([<sup>18</sup>F]-2-(3-fluoro-4-(methylamino)phenyl)benzo[d]thiazol-6-ol),<sup>8</sup> and two stilbene derivatives with fluorinated polyethylene glycol (PEG) units, [<sup>18</sup>F]BAY94-9172 ([<sup>18</sup>F]-4-(*N*-methylamino)-4'-(2-(2-(2-fluoroethoxy)ethoxy)ethoxy)stilbene)<sup>9,10</sup> and [<sup>18</sup>F]AV-45 ([<sup>18</sup>F]-(*E*)-4-(2-(6-(2-(2-(2-fluoroethoxy)ethoxy)ethoxy)ethyl)phenyl)stilbene).

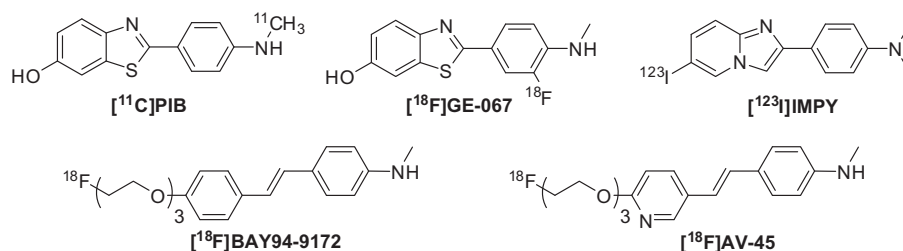


Figure 1. Chemical structure of  $A\beta$  imaging probes in clinical trials.

\* Corresponding authors. Tel.: +81 75 753 4608; fax: +81 75 753 4568 (M.O.), tel.: +81 75 753 4556; fax: +81 75 753 4568 (H.S.).

E-mail addresses: ono@pharm.kyoto-u.ac.jp (M. Ono), hsaji@pharm.kyoto-u.ac.jp (H. Saji).

oxy)ethoxy)ethoxy)pyridin-3-yl)vinyl)-*N*-methylaniline),<sup>11–13</sup> are being evaluated in phase II and phase III clinical trials. In addition, an iodine-123-labeled agent, [<sup>123</sup>I]IMPY ([<sup>123</sup>I]-6-iodo-2-(4'-dimethylamino-)phenyl-imidazo[1,2]pyridine) is the first SPECT probe to be evaluated in humans (Fig. 1).<sup>14–16</sup> However, a poor signal-to-noise ratio makes it difficult to distinguish AD patients.

In a search for novel A $\beta$  imaging probes, we have found that chalcone derivatives displayed excellent affinity for A $\beta$  aggregates, with some of them showing good uptake into and rapid clearance from the brain.<sup>17–19</sup> By selectively fixing the ketone part of the chalcone through an oxygen atom, we obtained a series of iodine-125-labeled aurone derivatives (Fig. 2), which showed high binding to A $\beta$  aggregates.<sup>20</sup> Notably, the PEGylated aurone derivatives displayed improved pharmacokinetics in vivo, and may served as potential A $\beta$  imaging probes for SPECT.<sup>21</sup> However, the conjugated double bonds in the chalcone and aurone structure may form *cis*-*trans* isomers. Herein, we report a series of benzofuran-2-yl(phenyl)methanone derivatives with a fixed double bond of chalcone as novel A $\beta$  imaging agents (Fig. 2). This is the first time benzofuran-2-yl(phenyl)methanone derivatives have been proposed as A $\beta$  imaging probes for detecting AD.

## 2. Results and discussion

### 2.1. Chemistry

The synthesis of benzofuran-2-yl(phenyl)methanone derivatives was readily accomplished by the reactions shown in Schemes

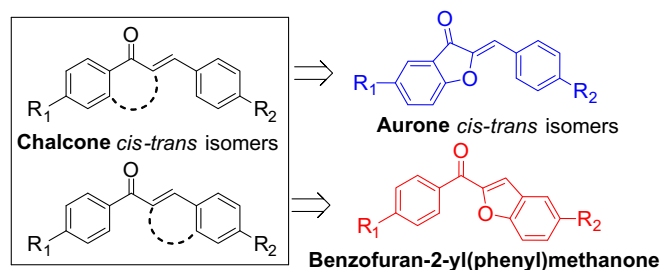
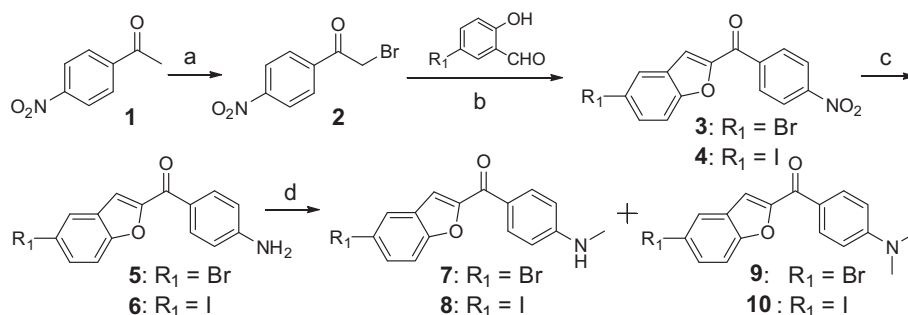
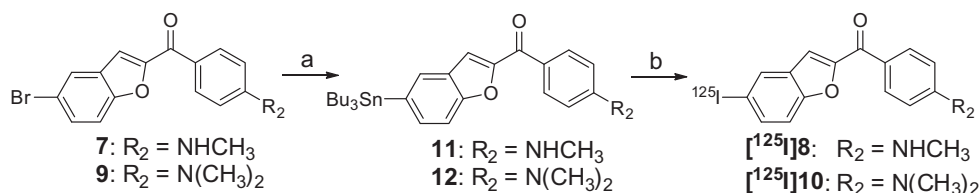


**Figure 2.** Design strategy of the benzofuran-2-yl(phenyl)methanone derivatives as probes for A $\beta$  plaques.



**Scheme 1.** Reagents and conditions: (a) Br<sub>2</sub>, Et<sub>2</sub>O, 0 °C, rt; (b) acetone, K<sub>2</sub>CO<sub>3</sub>, rt; (c) SnCl<sub>2</sub>, EtOH, HCl, reflux; (d) acetone, CH<sub>3</sub>I, K<sub>2</sub>CO<sub>3</sub>.



**Scheme 2.** Reagents and conditions: (a) (Bu<sub>3</sub>Sn)<sub>2</sub>(PPh<sub>3</sub>)<sub>4</sub>Pd, dioxane, Et<sub>3</sub>N, reflux; (b) [<sup>125</sup>I]NaI, HCl (1M), H<sub>2</sub>O<sub>2</sub> (3%), rt.

1 and 2. The  $\alpha$ -bromination of 4-nitroacetophenone (**1**) with bromine in ethylether under room temperature afforded **2** in an excellent yield of 94%. Formation of the benzofuran-2-yl(phenyl)methanone backbone was achieved by a Rap–Stoermer condensation reaction between the substituted salicylaldehyde and  $\alpha$ -haloacetophenone mediated by K<sub>2</sub>CO<sub>3</sub> in acetone at room temperature. Compounds **3** and **4** were obtained in good chemical yields (84% and 87%, respectively). The free amino derivatives **5** and **6** were obtained by reducing a nitro group to an amino group with SnCl<sub>2</sub> in ethanol under reflux condition (90% and 81%, respectively). Conversion of the amino derivatives **5** and **6** to the *N*-methylamino or *N,N*-dimethylamino derivatives was achieved by methylation with CH<sub>3</sub>I under alkaline conditions in one step. The desired tributyltin precursors **11** and **12** were prepared by Pd(PPh<sub>3</sub>)<sub>4</sub>-catalyzed trans-stannylation from their bromide compounds (18% and 29%, respectively).

### 2.2. Binding assay in vitro using A $\beta$ <sub>1–42</sub> aggregates

The affinity ( $K_i$ , nM) of the newly synthesized benzofuran-2-yl(phenyl)methanone derivatives were first evaluated by in vitro competitive binding assays with [<sup>125</sup>I]IMPY for aggregates of A $\beta$ <sub>1–42</sub> fibers in solution.<sup>15</sup> IMPY and [<sup>125</sup>I]IMPY were prepared based on previously reported procedures,<sup>15</sup> and IMPY was also screened under the same assay system for comparison. The derivatives inhibited the binding of [<sup>125</sup>I]IMPY to A $\beta$ <sub>1–42</sub> fibers in a dose-dependent manner, indicating an affinity for A $\beta$  aggregates (Fig. 3). As shown in Table 1, the tertiary *N,N*-dimethylamino analogues **9** and **10** were found to have higher affinity ( $K_i$  = 8.8 and 6.6 nM, respectively) than the secondary *N*-methylamino analogues **7** and **8**, while the corresponding primary amino analogues **5** and **6** showed low affinity ( $K_i$  = 156.6 and 133.2 nM, respectively), which is consistent with previous data on primary, secondary, and tertiary amino ligands.<sup>5</sup> Compounds **3** and **4** containing an electron-withdrawing group (NO<sub>2</sub>) had markedly reduced affinity ( $K_i$  >1000 nM). No significant difference was observed in binding between bromo and iodo derivatives. On the basis of the encouraging data obtained for the iodinated derivatives **8** ( $K_i$  = 34.5 nM) and **10** ( $K_i$  = 6.6 nM), these two ligands were chosen for radio-labeling and further biological evaluations.

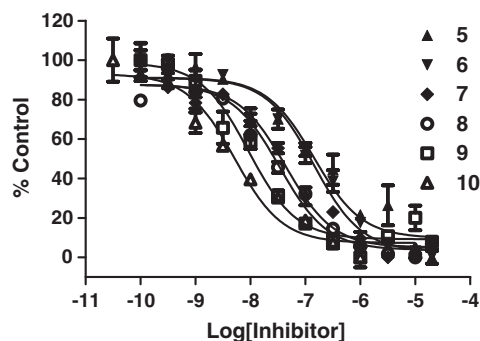


**Figure 3.** Inhibition curves of compounds 5–10 for  $A\beta_{1-42}$  aggregates V.S  $[^{125}I]$ IMPY.

**Table 1**  
Inhibition constants ( $K_i$ , nM) of compounds for the binding of  $[^{125}I]$ IMPY to  $A\beta_{1-42}$  aggregates

Compound	R <sub>1</sub>	R <sub>2</sub>	$K_i^a$ (nM)
3	Br	NO <sub>2</sub>	>1000
4	I	NO <sub>2</sub>	>1000
5	Br	NH <sub>2</sub>	156.6 ± 23.3
6	I	NH <sub>2</sub>	133.2 ± 10.4
7	Br	NHCH <sub>3</sub>	44.9 ± 9.7
8	I	NHCH <sub>3</sub>	34.5 ± 7.3
9	Br	N(CH <sub>3</sub> ) <sub>2</sub>	8.8 ± 3.9
10	I	N(CH <sub>3</sub> ) <sub>2</sub>	6.6 ± 1.0
IMPY	—	—	10.5 ± 1.0

<sup>a</sup> Values are the mean for three independent experiments.

### 2.3. Radiolabeling

The desired radioiodinated ligands  $[^{125}I]$ 8 and  $[^{125}I]$ 10 were successfully prepared from the corresponding tributyltin precursors through standard iododestannylation reactions, using sodium  $[^{125}I]$ iodide, hydrogen peroxide, and hydrochloric acid (Scheme 2). The overall radiochemical yield for  $[^{125}I]$ 8 and  $[^{125}I]$ 10 was 83.5% and 34.1%, respectively. The radiochemical identity of the  $^{125}I$ -labeled ligands was confirmed by co-injection with nonradioactive compounds on HPLC profiles (Fig. 4). The radiochemical purity of the purified ligands was greater than 97% and all had high specific activity (no carrier added, approx. 2200 Ci/mmol).

### 2.4. Autoradiography in vitro using AD transgenic mouse brain sections

Autoradiography in vitro using sections of brain tissue from double transgenic mice was selected for characterizing the specific binding of these radioiodinated ligands to  $A\beta$  plaques. As shown in Figure 5,  $[^{125}I]$ 10 showed excellent binding to  $A\beta$  plaques in the brain sections with numerous signals in the cortex region and minimal background labeling (Fig. 5A). The same section was also stained with thioflavin-S, a dye commonly used for  $A\beta$  plaques, and the distribution of  $A\beta$  plaques was consistent with the results of autoradiography (Fig. 5B, red arrow). However, the *N*-methylamino ligand,  $[^{125}I]$ 8, displayed less intense labeling (data not shown). This could be due to the lower affinity ( $K_i = 34.5$  nM) of 8 than that of 10. Therefore, we abandoned this *N*-methylamino ligand and focused only on  $[^{125}I]$ 10.

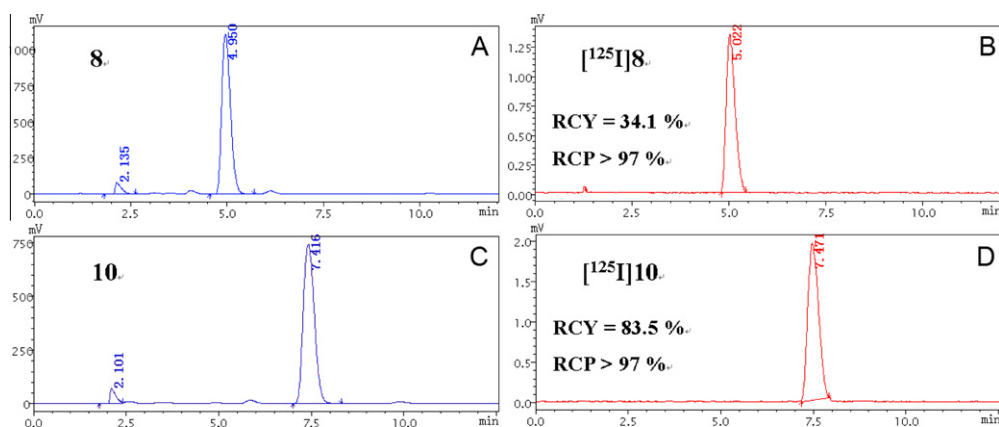


**Figure 4.** HPLC profiles of 8 (A),  $[^{125}I]$ 8 (B) and 10 (C),  $[^{125}I]$ 10 (D). HPLC conditions: Cosmosil C<sub>18</sub> column (Nacalai Tesque, 5C<sub>18</sub>-AR-II, 4.6 mm × 150 mm), CH<sub>3</sub>CN/H<sub>2</sub>O = 75/25, 1 mL/min, UV, 254 nm, 8tR (UV) = 4.95 min,  $[^{125}I]$ 8tR (RI) = 5.02 min and 10tR (UV) = 7.42 min,  $[^{125}I]$ 10tR (RI) = 7.47 min.

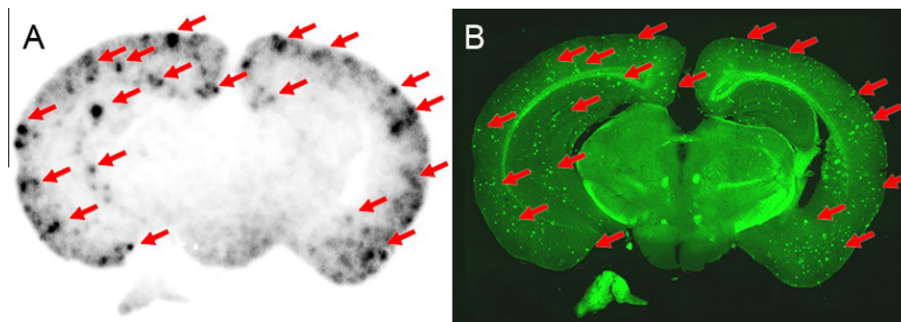


**Figure 5.** In vitro autoradiography of  $[^{125}I]$ 10 in a brain section of AD model mice (C57, APP/PS1, 12 months) (A). The same section was also stained with thioflavin-S (B) and the distribution of  $A\beta$  plaques was consistent with the results of autoradiography (red arrows).

**Table 2**  
Biodistribution in normal ddy mice after i.v. injection of [<sup>125</sup>I]**10** and the lipophilicity (log *D*) of the ligand<sup>a</sup>

Organ	[ <sup>125</sup> I] <b>10</b> log <i>D</i> = 4.40 ± 0.30				
	2 min	15 min	30 min	60 min	120 min
Blood	2.56 ± 0.25	1.16 ± 0.19	1.07 ± 0.29	0.82 ± 0.13	0.63 ± 0.15
Brain	3.53 ± 0.24	2.38 ± 0.39	1.51 ± 0.25	0.87 ± 0.15	0.41 ± 0.11
Heart	7.01 ± 0.86	1.45 ± 0.23	1.15 ± 0.41	0.74 ± 0.26	0.49 ± 0.08
Liver	16.19 ± 2.28	11.00 ± 1.13	6.70 ± 1.42	5.09 ± 0.74	3.59 ± 0.53
Spleen	2.75 ± 0.71	1.59 ± 0.32	0.94 ± 0.34	0.66 ± 0.02	0.43 ± 0.09
Lung	7.34 ± 1.90	2.20 ± 0.31	1.61 ± 0.38	0.94 ± 0.13	0.79 ± 0.20
Kidney	10.26 ± 1.52	3.84 ± 0.86	4.28 ± 1.18	1.90 ± 0.09	1.64 ± 0.39
Stomach <sup>b</sup>	0.95 ± 0.05	1.54 ± 0.61	2.60 ± 0.31	3.10 ± 0.51	3.76 ± 0.29
Intestine	3.14 ± 0.18	11.77 ± 2.12	21.81 ± 3.08	20.88 ± 3.90	25.19 ± 3.69
Thyroid <sup>b</sup>	0.02 ± 0.01	0.05 ± 0.02	0.18 ± 0.07	0.46 ± 0.09	0.80 ± 0.37

<sup>a</sup> Expressed as % injected dose per gram. Average for five mice ± standard deviation.

<sup>b</sup> Expressed as % injected dose per organ.

## 2.5. Biodistribution experiments with normal mice

To evaluate the kinetic properties of [<sup>125</sup>I]**10** in vivo, biodistribution experiments were performed in normal mice. As shown in Table 2, the *N,N*-dimethylamino ligand [<sup>125</sup>I]**10** displayed good penetration of the blood–brain barrier with an initial brain uptake of 3.53% ID/g at 2 min post-injection. Since there are no Aβ plaques in normal mice, the level of radioactivity in the brain decreased rapidly, being 0.87% ID/g at 60 min. In addition, the blood background during the experiment was low compared with the brain uptake, which is better for reducing nonspecific binding. The ratio brain<sub>2 min</sub>/brain<sub>30 min</sub> is considered an important index for selecting tracers with appropriate kinetics in vivo. [<sup>125</sup>I]**10** showed a brain<sub>2 min</sub>/brain<sub>30 min</sub> ratio of 2.34. Compared with radioiodinated *N,N*-dimethylamino chalcones (4.16) and aurones (7.27) reported previously,<sup>17,21</sup> [<sup>125</sup>I]**10** had superior initial brain uptake (3.53% ID/g) but the ratio of brain<sub>2 min</sub>/brain<sub>30 min</sub> (2.34) was lower, which may be due to its high lipophilicity (log *D* = 4.40 ± 0.30). As can be expected from the relatively high log *D* value, [<sup>125</sup>I]**10** was excreted predominantly by the hepatobiliary system. The hepatobiliary excretion to the intestines was also rather fast, and radioactivity was observed to accumulate within the intestine at later time points (25.19% ID/g at 120 min p.i.). Consistently, the accumulation of radioactivity in the thyroid increased gradually with time, suggesting that [<sup>125</sup>I]**10** was not stable to in vivo deiodination.

## 3. Conclusions

In conclusion, we successfully synthesized and evaluated a series of benzofuran-2-yl(phenyl)methanone derivatives by Rap–Stoermer condensation as probes for Aβ plaques. The *N,N*-dimethylamino and *N*-methylamino ligands displayed high affinity for Aβ aggregates in a binding assay in vitro. When labeled with <sup>125</sup>I, the *N,N*-dimethylamino derivative **10** showed specific labeling of Aβ plaques in the brain sections of AD model mice. In addition, [<sup>125</sup>I]**10** displayed good uptake into and moderate washout from the brain after injections in normal mice. Taken together, the present results suggest the novel benzofuran-2-yl(phenyl)methanone derivatives to be useful probes for detecting Aβ plaques in the AD brain.

## 4. Experimental section

### 4.1. General information

All the chemicals used were commercial products employed without further purification. The <sup>1</sup>H NMR spectra were obtained at 400 MHz on JEOL JNM-AL400 NMR spectrometers in CDCl<sub>3</sub> solutions at room temperature with TMS as an internal standard.

Chemical shifts are reported as δ values relative to the internal TMS. Coupling constants are reported in Hertz. Multiplicity is defined by s (singlet), d (doublet), t (triplet), and m (multiplet). Mass spectra were acquired with Shimadzu GC–MS–QP2010 Plus (APCI). HPLC was performed with a Shimadzu system (a LC-10AT pump with a SPD-10A UV detector, λ = 254 nm) using a column of Cosmosil C<sub>18</sub> (Nacalai Tesque, 5C<sub>18</sub>-AR-II, 4.6 mm × 150 mm) and acetonitrile/water = 75/25 as the mobile phase at a flow rate of 1.0 mL/min. All key compounds were proven by this method to show ≥95% purity (see supplementary data).

### 4.2. 2-Bromo-1-(4-nitrophenyl)ethanone (2)

To a solution of **1** (1.65 g, 10 mmol) in dry ethylether (150 mL) was added Br<sub>2</sub> (1.60 g, 10 mmol) dropwise in an ice bath. The reaction mixture was stirred at room temperature for 2 h. Evaporation of the solvent afforded 2.29 g of **2** as a white crystal (94%). <sup>1</sup>H NMR (400 MHz, CDCl<sub>3</sub>) δ 8.35 (d, *J* = 9.1 Hz, 2H), 8.15 (d, *J* = 9.1 Hz, 2H), 4.47 (s, 2H).

### 4.3. (5-Bromobenzofuran-2-yl)(4-nitrophenyl)methanone (3)

A mixture of **2** (488 mg, 2 mmol), 5-bromosalicylaldehyde (402 mg, 2 mmol), and K<sub>2</sub>CO<sub>3</sub> (276 mg, 2 mmol) in acetone (10 mL) was stirred at room temperature for 8 h, and the reaction mixture was washed with water to give **3** in 84% yield (580 mg). <sup>1</sup>H NMR (400 MHz, CDCl<sub>3</sub>) δ 8.41 (d, *J* = 8.9 Hz, 2H), 8.23 (d, *J* = 8.9 Hz, 2H), 7.91 (d, *J* = 1.9 Hz, 1H), 7.65 (dd, *J* = 8.8, 2.0 Hz, 1H), 7.56 (d, *J* = 0.9 Hz, 1H), 7.54 (dd, *J* = 8.8, 0.4 Hz, 1H). HRMS (EI): *m/z* calcd for C<sub>15</sub>H<sub>8</sub>BrNO<sub>4</sub> 344.9629; found 344.9636.

### 4.4. (5-Iodobenzofuran-2-yl)(4-nitrophenyl)methanone (4)

The reaction described for **3** was used, and **4** was obtained in a yield of 87%. <sup>1</sup>H NMR (400 MHz, CDCl<sub>3</sub>) δ 8.41 (d, *J* = 8.7 Hz, 2H), 8.22 (d, *J* = 8.6 Hz, 2H), 8.12 (d, *J* = 1.7 Hz, 1H), 7.81 (dd, *J* = 8.8, 1.7 Hz, 1H), 7.54 (d, *J* = 0.8 Hz, 1H), 7.43 (dd, *J* = 8.8, 0.8 Hz, 1H). HRMS (EI): *m/z* calcd for C<sub>15</sub>H<sub>8</sub>INO<sub>4</sub> 392.9491; found 392.9498.

### 4.5. (4-Aminophenyl)(5-bromobenzofuran-2-yl)methanone (5)

A mixture of **3** (344 mg, 1.0 mmol) and SnCl<sub>2</sub> (380 mg, 2.0 mmol) dissolved in 50 mL of ethanol containing 2 mL of concentrated hydrochloric acid was stirred under reflux for 2 h. After the mixture had cooled to room temperature, 2 M NaOH (100 mL) was added and extracted with ethyl acetate (100 mL). The organic layer was dried over Na<sub>2</sub>SO<sub>4</sub>. The filtrate was concentrated to give 283 mg of **5** (90%). <sup>1</sup>H NMR (400 MHz, CDCl<sub>3</sub>) δ 8.01 (dd, *J* = 8.7, 1.0 Hz, 2H), 7.90–7.81 (m, 1H), 7.55 (ddt, *J* = 4.1, 2.2, 1.1 Hz, 1H), 7.50 (d, *J* = 8.8 Hz, 1H), 7.42 (s, 1H), 6.73 (dd, *J* = 8.7,

0.9 Hz, 2H), 4.25 (s, 2H). HRMS (EI):  $m/z$  calcd for  $C_{15}H_{10}BrNO_2$  314.9889; found 314.9894.

#### 4.6. (4-Aminophenyl)(5-iodobenzofuran-2-yl)methanone (6)

The reaction described for **5** was used, and **6** was obtained in a yield of 81%.  $^1H$  NMR (400 MHz,  $CD_3OD$ )  $\delta$  8.15 (d,  $J = 1.5$  Hz, 1H), 7.94 (d,  $J = 8.8$  Hz, 2H), 7.77 (dd,  $J = 8.7, 1.8$  Hz, 1H), 7.51 (d,  $J = 0.9$  Hz, 1H), 7.46 (d,  $J = 8.8$  Hz, 1H), 6.72 (d,  $J = 8.8$  Hz, 2H), 4.85 (s, 2H). HRMS (EI):  $m/z$  calcd for  $C_{15}H_{10}INO_2$  362.9752; found 362.9756.

#### 4.7. (5-Bromobenzofuran-2-yl)(4-(methylamino)phenyl)methanone (7)

To a solution of **5** (315 mg, 1 mmol) in acetone (15 mL) was added  $CH_3I$  (0.18 mL, 3 mmol) and anhydrous  $K_2CO_3$  (138 mg, 1 mmol). The reaction mixture was stirred at room temperature for 12 h and poured into water. The mixture was extracted with ethyl acetate. The organic layers were combined and dried over  $Na_2SO_4$ . Evaporation of the solvent afforded a residue, which was purified by silica gel chromatography to give 108 mg of **7** (33%).  $^1H$  NMR (400 MHz,  $CDCl_3$ )  $\delta$  8.06 (d,  $J = 9.0$  Hz, 2H), 7.85 (dd,  $J = 1.9, 0.5$  Hz, 1H), 7.55 (dd,  $J = 8.8, 1.9$  Hz, 1H), 7.52–7.48 (m, 1H), 7.41 (d,  $J = 0.9$  Hz, 1H), 6.65 (d,  $J = 8.9$  Hz, 2H), 4.49 (s, 1H), 2.95 (s, 3H). HRMS (EI):  $m/z$  calcd for  $C_{16}H_{12}BrNO_2$  329.0042; found 329.0051.

#### 4.8. (5-Iodobenzofuran-2-yl)(4-(methylamino)phenyl)methanone (8)

The reaction described for **7** was used, and **8** was obtained in a yield of 41%.  $^1H$  NMR (400 MHz,  $CDCl_3$ )  $\delta$  8.03 (d,  $J = 1.8$  Hz, 1H), 8.03 (d,  $J = 8.9$  Hz, 2H), 7.70 (dd,  $J = 8.8, 1.2$  Hz, 1H), 7.44–7.29 (m, 2H), 6.63 (d,  $J = 8.9$  Hz, 2H), 2.92 (s, 3H). HRMS (EI):  $m/z$  calcd for  $C_{16}H_{12}INO_2$  376.9904; found 376.9913.

#### 4.9. (5-Bromobenzofuran-2-yl)(4-(dimethylamino)phenyl)methanone (9)

The reaction described for **7** was used, and **9** was obtained in a yield of 26%.  $^1H$  NMR (400 MHz,  $CDCl_3$ )  $\delta$  8.10 (d,  $J = 9.2$  Hz, 2H), 7.85 (d,  $J = 1.7$  Hz, 1H), 7.54 (dd,  $J = 8.8, 1.7$  Hz, 1H), 7.50 (d,  $J = 8.8$  Hz, 1H), 7.41 (d,  $J = 0.8$  Hz, 1H), 6.74 (d,  $J = 9.1$  Hz, 2H), 3.11 (s, 6H). HRMS (EI):  $m/z$  calcd for  $C_{17}H_{14}BrNO_2$  343.0200; found 343.0207.

#### 4.10. (4-(Dimethylamino)phenyl)(5-iodobenzofuran-2-yl)methanone (10)

The reaction described for **7** was used, and **10** was obtained in a yield of 37%.  $^1H$  NMR (400 MHz,  $CDCl_3$ )  $\delta$  8.10 (d,  $J = 9.0$  Hz, 2H), 8.05 (s, 1H), 7.71 (d,  $J = 8.7$  Hz, 1H), 7.40 (d,  $J = 8.7$  Hz, 1H), 7.39 (s, 1H), 6.74 (d,  $J = 9.1$  Hz, 2H), 3.11 (s, 6H). HRMS (EI):  $m/z$  calcd for  $C_{17}H_{14}INO_2$  391.0061; found 391.0069.

#### 4.11. (4-(Methylamino)phenyl)(5-(tributylstannyl)benzofuran-2-yl)methanone (11)

A mixture of **7** (165 mg, 0.5 mmol),  $(Bu_3Sn)_2$  (0.5 mL), and  $(Ph_3P)_4Pd$  (60 mg, 0.04 mmol) in a mixed solvent (10 mL, 4:1 dioxane/ $Et_3N$ ) was stirred under reflux for 10 h. The solvent was removed, and the residue was purified by silica gel chromatography to give 48 mg of **11** (18%).  $^1H$  NMR (400 MHz,  $CDCl_3$ )  $\delta$  8.07 (d,  $J = 8.6$  Hz, 2H), 7.79 (s, 1H), 7.61 (d,  $J = 8.1$  Hz, 1H), 7.52 (d,  $J = 8.1$  Hz, 1H), 7.47 (s, 1H), 6.64 (d,  $J = 8.6$  Hz, 2H),

4.36 (s, 1H), 2.95 (s, 3H), 1.82–0.57 (m, 27H). MS (APCI):  $m/z$  calcd for  $C_{28}H_{39}NO_2Sn$  541.20; found 542.30 ( $M+H^+$ ).

#### 4.12. (4-(Dimethylamino)phenyl)(5-(tributylstannyl)benzofuran-2-yl)methanone (12)

The reaction described for **11** was used, and **12** was obtained in a yield of 29%.  $^1H$  NMR (400 MHz,  $CDCl_3$ )  $\delta$  8.11 (d,  $J = 8.8$  Hz, 2H), 7.80 (s, 1H), 7.61 (d,  $J = 8.1$  Hz, 1H), 7.52 (d,  $J = 8.1$  Hz, 1H), 7.47 (s, 1H), 6.74 (d,  $J = 8.9$  Hz, 2H), 3.10 (s, 6H), 1.69–0.76 (m, 27H). MS (APCI):  $m/z$  calcd for  $C_{29}H_{41}NO_2Sn$  555.22; found 556.30 ( $M+H^+$ ).

#### 4.13. Radiolabeling

The radioiodinated ligands [ $^{125}I$ ]**8** and [ $^{125}I$ ]**10** were prepared from the corresponding tributyltin precursor through an iododestannylation reaction according to a procedure described previously with some modifications.<sup>17</sup> Briefly, 50  $\mu$ L of  $H_2O_2$  (3%) was added to a mixture of a tributyltin derivative (0.1 mg/100  $\mu$ L in ethanol), 200  $\mu$ Ci of sodium [ $^{125}I$ ]iodide (specific activity 2200 Ci/mmol), and 100  $\mu$ L of 1 M HCl in a sealed vial. The reaction was allowed to proceed at room temperature for 15 min and then quenched with the addition of 50  $\mu$ L of a saturated  $NaHSO_3$  solution. The reaction mixture was extracted with ethyl acetate ( $3 \times 1$  mL) after neutralization with 10 mg of sodium bicarbonate. The combined extracts were evaporated dry. The residues were dissolved in 100  $\mu$ L of EtOH and purified by HPLC using a 5C<sub>18</sub>-AR-II analytical column ( $4.6 \times 150$  mm),  $CH_3CN/H_2O = 3/1$ , at a flow rate of 1.0 mL/min. The desired fractions containing the product were evaporated dry and redissolved in 100% ethanol. Finally, the radiochemical identity of [ $^{125}I$ ]**8** and [ $^{125}I$ ]**10** was verified by co-injection with nonradioactive compounds by HPLC. The final product was stored at  $-20$  °C until use for autoradiography and biodistribution experiments.

#### 4.14. Binding assay in vitro using $A\beta_{1-42}$ aggregates

Inhibition experiments were carried out in  $12 \times 75$  mm borosilicate glass tubes according to a procedure described previously with some modifications.<sup>22</sup> One hundred microliters of aggregated  $A\beta$  fibrils (60 nM in the final assay mixture) was added to a mixture containing 100  $\mu$ L of radioligand ([ $^{125}I$ ]IMPY) of the appropriate concentration, 10  $\mu$ L of inhibitor ( $10^{-5}$ – $10^{-10}$  M in ethanol), and 790  $\mu$ L of PBS (0.2 M, pH 7.4) in a final volume of 1 mL. Nonspecific binding was defined in the presence of 1  $\mu$ M IMPY. The mixture was incubated for 2 h at 37 °C with constant shaking, then the bound and free radioactivity were separated by vacuum filtration through borosilicate glass fiber filters (Whatman GF/B) using a cell harvester (Brandel, M-24 Gaithersburg, MD, USA). Filters containing the bound [ $^{125}I$ ] ligand were measured for radioactivity in a  $\gamma$ -counter (WALLAC/Wizard 1470, USA) with 70% counting efficiency. Under the assay conditions, the specifically bound fraction accounted for about 10% of all the radioactivity. The half maximal inhibitory concentration ( $IC_{50}$ ) was determined using GRAPHPAD PRISM 4.0, the inhibition constant ( $K_i$ ) was calculated using the Cheng-Prusoff equation:  $K_i = IC_{50}/(1 + [L]/K_d)$ .<sup>23</sup>

#### 4.15. Autoradiography in vitro using AD transgenic mouse brain sections

Paraffin-embedded brain sections of AD model mice (C57, APP/PS1, 12 months) were used for autoradiography. The sections were deparaffinized with  $2 \times 20$  min washes in xylene;  $2 \times 5$  min washes in 100% ethanol; a 5 min wash in 90% ethanol/ $H_2O$ ; a 5 min wash in 80% ethanol/ $H_2O$ ; a 5 min wash in 60% ethanol/ $H_2O$  and a 10 min wash in running tap water, and then incubated

in PBS (0.2 M, pH 7.4) for 30 min. The sections were incubated with radiotracers (5  $\mu$ Ci/100  $\mu$ L) for 1 h at room temperature. They were then washed with 40% ethanol for 3 min, and rinsed with water for 30 s. After drying, the  $^{125}$ I-labeled sections were exposed to a Fuji Film imaging plate overnight. The in vitro autoradiographic images were obtained using a BAS5000 scanner system (Fuji Film). The presence and location of plaques in the sections were confirmed by fluorescent staining with thioflavin-S (1  $\mu$ M).

#### 4.16. Biodistribution experiments with normal mice

The biodistribution experiments were performed in normal ddY mice (female, 5 weeks) and approved by the animal care committee of Kyoto University. A saline solution (100  $\mu$ L, 5% EtOH) containing [ $^{125}$ I]10 (0.9  $\mu$ Ci) was injected directly into the tail vein. The mice were sacrificed at various time points post-injection. The organs of interest were removed and weighed, and the radioactivity was measured with an automatic  $\gamma$ -counter. The percentage dose per gram of wet tissue was calculated by a comparison of the tissue counts to suitably diluted aliquots of the injected material.

#### 4.17. Determination of the partition co-efficient

The partition co-efficient of the radioligand was determined as described previously but with some modifications.<sup>17</sup> Radioligand (10  $\mu$ Ci) was added to premixed suspensions containing 3 g of *n*-octanol and 3 g of PBS (0.05 M, pH 7.4) in a test tube. The test tube was vortexed for 3 min at room temperature, and centrifuged for 5 min at 3000 rpm. Two weighted samples from the *n*-octanol (50  $\mu$ L) and buffer (800  $\mu$ L) layers were measured. The partition co-efficient was expressed as the logarithm of the ratio of the counts per gram from *n*-octanol versus PBS. Samples from the *n*-octanol layer were repartitioned until consistent partitions of co-efficient values were obtained. The measurement was done in triplicate and repeated three times.

#### Acknowledgments

This study was supported by the Funding Program for Next Generation World-Leading Researchers, and a Grant-in-aid for Young Scientists (A) and Exploratory Research from the Ministry of Education, Culture, Sports, Science and Technology, Japan. This study was also supported by the China Scholarship Council (CSC).

#### Supplementary data

Supplementary data associated with this article can be found, in the online version, at doi:10.1016/j.bmc.2011.04.049.

#### References and notes

- Selkoe, D. J. *JAMA-J. Am. Med. Assoc.* **2000**, *283*, 1615.
- Selkoe, D. J. *Physiol. Rev.* **2001**, *81*, 741.
- Hardy, J. A.; Selkoe, D. J. *Science* **2002**, *297*, 353.
- Mathis, C. A.; Wang, Y.; Klunk, W. E. *Curr. Pharm. Des.* **2004**, *10*, 1469.
- Cai, L. S.; Innis, R. B.; Pike, V. W. *Curr. Med. Chem.* **2007**, *14*, 19.
- Mathis, C. A.; Wang, Y.; Holt, D. P.; Huang, G. F.; Debnath, M. L.; Klunk, W. E. *J. Med. Chem.* **2003**, *46*, 2740.
- Klunk, W. E.; Engler, H.; Nordberg, A.; Wang, Y.; Blomqvist, G.; Holt, D. P.; Bergstrom, M.; Savitcheva, I.; Huang, G. F.; Estrada, S.; Ausen, B.; Debnath, M. L.; Barletta, J.; Price, J. C.; Sandell, J.; Lopresti, B. J.; Wall, A.; Koivisto, P.; Antoni, G.; Mathis, C. A.; Langstrom, B. *Ann. Neurol.* **2004**, *55*, 306.
- Koole, M.; Lewis, D.; Buckley, C.; Nelissen, N.; Vandenbulcke, M.; Brooks, D. J.; Vandenbergh, R.; Laere, K. V. *J. Nucl. Med.* **2009**, *50*, 818.
- Rowe, C. C.; Ackerman, U.; Browne, W.; Mulligan, R.; Pike, K. L.; O'Keefe, G.; Tochon-Danguy, H.; Chan, G.; Berlangieri, S. U.; Jones, G.; Dickinson-Rowe, K. L.; Kung, H. F.; Zhang, W.; Kung, M. P.; Skovronsky, D.; Dyrks, T.; Holl, G.; Krause, S.; Friebe, M.; Lehman, L.; Lindemann, S.; Dinkelborg, L. M.; Masters, C. L.; Villemagne, V. L. *Lancet Neurol.* **2008**, *7*, 129.
- Zhang, W.; Oya, S.; Kung, M. P.; Hou, C.; Maier, D. L.; Kung, H. F. *Nucl. Med. Biol.* **2005**, *32*, 799.
- Zhang, W.; Kung, M.-P.; Oya, S.; Hou, C.; Kung, H. F. *Nucl. Med. Biol.* **2007**, *34*, 89.
- Choi, S. R.; Golding, G.; Zhuang, Z. P.; Zhang, W.; Lim, N.; Hefti, F.; Benedum, T. E.; Kilbourn, M. R.; Skovronsky, D.; Kung, H. F. *J. Nucl. Med.* **2009**, *50*, 1887.
- Kung, H. F.; Choi, S. R.; Qu, W. C.; Zhang, W.; Skovronsky, D. *J. Med. Chem.* **2010**, *53*, 933.
- Kung, M. P.; Hou, C.; Zhuang, Z. P.; Zhang, B.; Skovronsky, D.; Trojanowski, J. Q.; Lee, V. M.; Kung, H. F. *Brain Res.* **2002**, *956*, 202.
- Zhuang, Z. P.; Kung, M. P.; Wilson, A.; Lee, C. W.; Plossl, K.; Hou, C.; Holtzman, D. M.; Kung, H. F. *J. Med. Chem.* **2003**, *46*, 237.
- Newberg, A. B.; Wintering, N. A.; Plossl, K.; Hochold, J.; Stabin, M. G.; Watson, M.; Skovronsky, D.; Clark, C. M.; Kung, M. P.; Kung, H. F. *J. Nucl. Med.* **2006**, *47*, 748.
- Ono, M.; Haratake, M.; Mori, H.; Nakayama, M. *Bioorg. Med. Chem.* **2007**, *15*, 6802.
- Ono, M.; Hori, M.; Haratake, M.; Tomiyama, T.; Mori, H.; Nakayama, M. *Bioorg. Med. Chem.* **2007**, *15*, 6388.
- Ono, M.; Watanabe, R.; Kawashima, H.; Cheng, Y.; Kimura, H.; Watanabe, H.; Haratake, M.; Saji, H.; Nakayama, M. *J. Med. Chem.* **2009**, *52*, 6394.
- Ono, M.; Maya, Y.; Haratake, M.; Ito, K.; Mori, H.; Nakayama, M. *Biochem. Biophys. Res. Commun.* **2007**, *361*, 116.
- Maya, Y.; Ono, M.; Watanabe, H.; Haratake, M.; Saji, H.; Nakayama, M. *Bioconjug. Chem.* **2009**, *20*, 95.
- Zhuang, Z. P.; Kung, M. P.; Hou, C.; Skovronsky, D. M.; Gur, T. L.; Plossl, K.; Trojanowski, J. Q.; Lee, V. M. Y.; Kung, H. F. *J. Med. Chem.* **2001**, *44*, 1905.
- Cheng, Y.; Prusoff, W. *Biochem. Pharmacol.* **1973**, *22*, 3099.